IEEE Photonics Journal
An IEEE Photonics Society Publication

Effect of Laser Coupling and Active Stabilization on the Phase Noise Performance of Optoelectronic Microwave Oscillators Based on Whispering-Gallery-Mode Resonators

Volume 7, Number 1, February 2015

Khaldoun Saleh
Guoping Lin
Yanne K. Chembo, Senior Member, IEEE

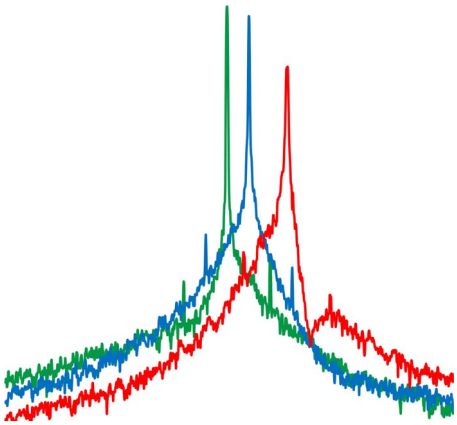

DOI: 10.1109/JPHOT.2014.2381661
1943-0655 © 2014 IEEE

Effect of Laser Coupling and Active Stabilization on the Phase Noise Performance of Optoelectronic Microwave Oscillators Based on Whispering-Gallery-Mode Resonators

Khaldoun Saleh, Guoping Lin, and Yanne K. Chembo, *Senior Member, IEEE*

FEMTO-ST Institute (UMR CNRS 6174), Optics Department, 25030 Besançon, France

DOI: 10.1109/JPHOT.2014.2381661

Manuscript received November 10, 2014; revised December 3, 2014; accepted December 4, 2014. Date of publication December 18, 2014; date of current version January 6, 2015. This work was supported by the European Research Council (ERC) through the NextPhase and Versyt Projects, by the Centre National d'Etudes Spatiales (CNES) through the SHYRO Project, by the Région de Franche-Comté, and by the Labex ACTION. Corresponding author: K. Saleh (e-mail: khaldoun.saleh@femto-st.fr).

Abstract: We investigate the effect of laser coupling efficiency and active stabilization on the phase noise performance of optoelectronic oscillators based on monocrystalline whispering-gallery-mode disk resonators. We show that the resonator's intrinsic optical quality factor is not the only parameter to optimize in order to get a good phase-noise performance. In addition, the oscillator setup may involve many noise conversion processes that have to be evaluated and understood in order to optimize the spectral purity of the output microwave. We study the effect of the laser lightwave coupling into and out of the optical resonator on the spectral purity of the oscillator, and we evidence the role of this critical parameter on the phase noise performance. We also investigate the upconversion of baseband noise, even originating from marginal components in the oscillator setup, onto the output microwave and the resulting degradation of the spectral purity. Our experimental results are obtained using two ultrahigh-Q disk resonators manufactured with calcium and magnesium fluoride, respectively.

Index Terms: Optoelectronic devices, optical resonators, whispering gallery modes, microwave oscillators, phase noise.

1. Introduction

The need for high spectral purity microwave sources featuring low close-in phase noise levels has become imperative for a wide range of applications over the past two decades. Among these applications, we can especially mention the communications systems (e.g., satellites and onboard signal distribution), time and frequency metrology, and radars. On the other hand, as it is commonly known, the quality factor of microwave resonators degrades when the application frequency (f_{RF}) increases. As a result, the spectral purity of a microwave oscillator based on such resonators will be degraded as well.

Fortunately, it has been proven in the early 1990s that optics can represent an elegant solution to attain high spectral purity in microwave oscillators through the so-called optoelectronic

oscillator (OEO) approach [1]. The particularity here is that an OEO is a microwave oscillator based on an optical stability element (optical energy storage element). In such oscillators, a few km-long optical fiber delay line (DL) can be used. Therefore, one can take benefit of the large optical delay provided by the DL featuring extremely low optical loss [2], [3]. Alternatively, because of DL's different drawbacks (e.g. system size, thermal stability, dispersion [4], nonlinear effects [5]–[7], spurious modes [8], [9], etc.), one can take benefit of the large optical storage time provided by a high-quality factor (Q) whispering gallery mode resonator (WGMR) [10]–[13].

In point of fact, a WGMR is by far much compact than a DL as its diameter is usually in the range of few millimeters or less. Besides that, multiple optical resonance combs/families are generated in a WGMR for both transverse electric (TE) and transverse magnetic (TM) modes because of the WGMR's tridimensional shape. Individually, under certain conditions, each optical mode of a resonance comb can act as a high selectivity band-pass optical filter in an OEO setup. Nevertheless, a WGMR also has drawbacks that have to be considered and carefully studied, especially if the WGMR is meant to be used as the stability element inside an OEO.

Indeed, an OEO is a complex system in which the WGMR's intrinsic optical Q ($Q_{\text{Opt-int}}$) is not the only parameter to optimize in order to get a good phase noise performance. In addition, the OEO setup may involve many noise conversion processes that have to be evaluated and understood. In this article, we present several investigations performed on an OEO based on two different monocrystalline disk-shaped WGMRs. These disk-resonators are made of calcium fluoride (CaF_2) and magnesium fluoride (MgF_2). The performance of the two WGMRs have been compared by firstly measuring their intrinsic quality factors and later on by measuring their microwave equivalent loaded quality factors (Q_{RF}) once included inside the OEO setup. Correspondingly, the RF and phase noise spectra of the OEO based each time on one of these WGMRs have been characterized. The measured RF and phase noise spectra are presented and discussed in detail. We also present a study on the performance of the OEO when different modes, belonging to different resonance combs generated in the CaF_2 WGMR, have been used. In addition, we investigate the source of the excess close-in phase noise peaks that are usually detected in the OEO's spectrum. The different procedures performed to identify the origin of these noise peaks and to finally reduce them are described. Moreover, we have studied the effect of the laser stabilization loop used to lock the laser wavelength onto an optical mode of the WGMR on the spectral purity of the OEO. The results of this study are also discussed in detail.

2. Characterization of the Whispering Gallery Mode Resonators

The two WGMRs we are using in this work are both disk-shaped and have both a 12 mm diameter (this value is the raw disk's diameter before the fabrication process, where grinding and polishing take place [14]). Both WGMRs have been first characterized in the optical domain in order to measure the $Q_{\text{Opt-int}}$ of a given optical mode of each WGMR. The family of each mode (i.e. the resonance comb/family to which the optical mode belongs to) is then accurately characterized in the microwave frequency domain.

In order to characterize a WGMR, the laser lightwave must be first coupled into the resonator (we use a Koheras fiber laser with sub-kilohertz linewidth). This is done using a tapered optical microfiber clamped on a xyz translation stage. The optical microfiber is used in our laser-WGMR coupling scheme because it enables whispering gallery modes to be efficiently excited in the resonator [15].

2.1. Intrinsic Quality Factor Measurement

For each WGMR, once a useful optical mode was identified amongst the different WGMR's eigenmodes (i.e., a best-critically coupled mode featuring a suitable free spectral range (FSR)), the mode's $Q_{\text{Opt-int}}$ was measured using the cavity ring down technique (CRD). This technique consists of measuring the photon lifetime inside a given resonant optical mode of the cavity, giving access to the mode's $Q_{\text{Opt-int}}$. Details on this measurement technique can be found in [16].

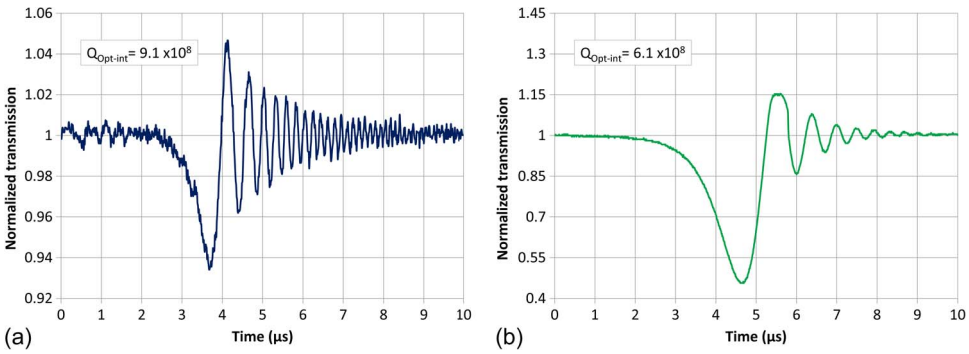

Fig. 1. CRD measurement for two selected optical modes respectively excited in (a) the CaF_2 WGMR and (b) the MgF_2 WGMR.

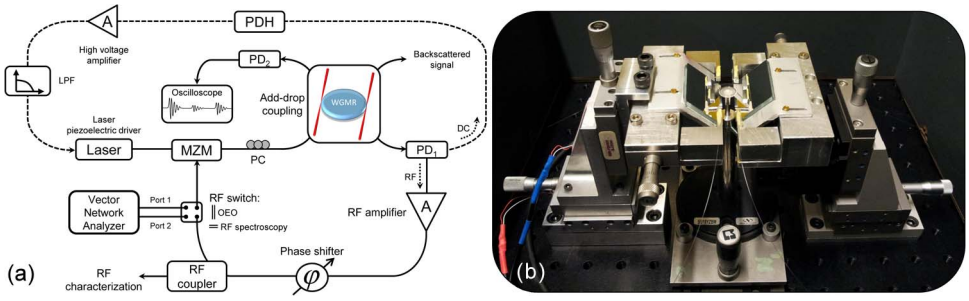

Fig. 2. (a) OEO experimental setup including the PDH laser stabilization loop. MZM: Mach-Zehnder modulator; PC: polarization controller; PD_1: fast photodiode; PD_2: slow photodiode; LPF: low pass filter. Two tapered optical microfibers are used in an add-drop configuration to couple the laser into and out of the WGMR by evanescent field. (b) Image of the laser-WGMR coupling bench using two combined micrometric-nanometric xyz translation stages.

Fig. 1 shows the results obtained using the CRD technique to characterize two selected optical modes, respectively excited in the CaF_2 and the MgF_2 WGMR while an add-only coupling configuration was used. From these CRD measurements we can infer a mode's $Q_{\text{Opt-int}}$ of 9.1×10^8 for the CaF_2 WGMR $(Q_{\text{Opt-int-CaF}_2})$ and a mode's $Q_{\text{Opt-int}}$ of 6.1×10^8 for the MgF_2 WGMR $(Q_{\text{Opt-int-MgF}_2})$.

2.2. Loaded Quality Factor Measurement

2.2.1. Experimental Setup

The scheme of the OEO setup we are using in this work is depicted in Fig. 2(a). Besides the OEO's optical and microwave components, a vector network analyzer (VNA; an ANRITSU 37369A VNA with 1 kHz frequency resolution) was added just before the Mach-Zehnder modulator (MZM). This has been done in order to measure the S_{21} transmission coefficient of the WGMR when it is incorporated inside the OEO's optoelectronic loop [12]. In addition, a four-port RF switch has been added to the setup to easily choose between the S_{21} transmission coefficient measurement configuration and the OEO oscillation configuration.

In order to include a WGMR inside the OEO loop, the laser lightwave has been coupled into and out of the WGMR by the evanescent field through two tapered optical microfibers in an add-drop configuration (see Fig. 2). It should be noted here that in the case of the CaF_2 WGMR, we were using two manual xyz translation stages with micrometric resolution in order to control the coupling between the input-output microfibers and the WGMR. Afterwards, in the case of the MgF_2 WGMR, two combined micrometric-nanometric *xyz* translation stages were adopted in

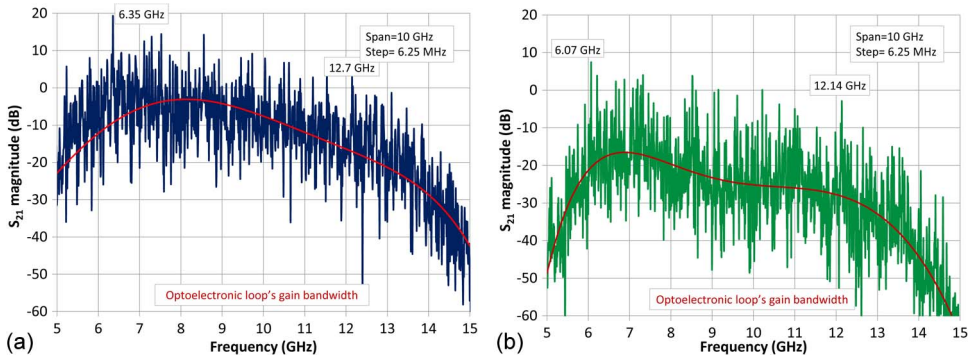

Fig. 3. Large scanning bandwidth S_{21} coefficient's magnitude measurement performed on (a) the CaF_2 WGMR and (b) the MgF_2 WGMR.

order to control the optical coupling with high precision. In such a scenario, the resolution of the coupling control has to be usually much less than the pumping laser's wavelength in order to correctly achieve an optimal coupling. Our combined micrometric-nanometric xyz translation stages, depicted in Fig. 2(b), consisted each of a manual xyz translation stage with micrometric resolution, on which we have mounted another xyz piezoelectric translation stage with nanometric resolution ($\approx$ 1 nm). Indeed, we have found that the optical coupling must be accurately controlled in order to take full advantage of the WGMR's high $Q_{\text{Opt-int}}$. Otherwise, the loaded WGMR performance will be affected and consequently the OEO based on this WGMR.

After a laser lightwave coupling into and out of the WGMR, its wavelength has been efficiently stabilized onto the identified optical mode by means of a Pound–Drever–Hall (PDH) laser stabilization technique. Details on this laser stabilization technique can be found in [17]. Using our final setup, it has been possible to fully characterize a given optical resonance comb when the laser carrier was locked onto the center of one of its optical modes. Indeed, the measurement of the S_{21} transmission coefficient gives access to the mode's loaded optical Q (Q_{Opt}) and the resonance comb's FSR.

2.2.2. Comparison of Optical Modes in the CaF_2 WGMR and the MgF_2 WGMR

In the case of a WGMR, the FSR mainly depends on the WGMR's circumference, and it is given by $FSR = c/2\pi nr$, where c is the speed of light, r is the radius of the WGMR, and n is the group-velocity index of the disk (at $\lambda = 1559$ nm, $n_{CaF_2} = 1.37$, and $n_{MgF_2} = 1.42$). Assuming perfectly circular disks with 12 mm diameters, the *FSRs* of the fundamental mode's family in the CaF_2 WGMR and the MgF_2 WGMR should be equal to 5.6 GHz and 5.8 GHz, respectively. Of course, one has to expect higher *FSRs* than the calculated ones because after all the fabrication steps, the WGMRs' diameters will be less than 12 mm.

Fig. 3 shows the results obtained when a S_{21} coefficient's magnitude measurement has been performed on the CaF_2 and the MgF_2 disks for large scanning bandwidths. In both cases, the measurement shows numerous optical modes related to the different optical resonance combs generated inside the WGMRs. In the CaF_2 WGMR, two modes, at 6.35 GHz from the laser carrier and its multiple at 12.7 GHz, are particularly interesting [see Fig. 3(a)]. This is because these two optical modes seem to belong to the same optical resonance comb and because the FSR is close the calculated fundamental FSR of the CaF_2 WGMR. Similarly, we can see in Fig. 3(b) that two modes at 6.07 GHz and its multiple at 12.14 GHz are generated in the MgF_2 WGMR.

When the S_{21} measurement is focused on a given optical mode we can get the information on its full width at half maximum (FWHM) and therefore on its Q_{Opt}. Here, it is noteworthy that the FWHM of the optical resonance is preserved in the microwave frequency domain. Therefore, the measured Q_{Opt} will have its equivalent loaded microwave Q (Q_{RF}) in the microwave frequency domain. This Q_{RF} can be easily derived by multiplying the measured Q_{Opt} by the RF to optical frequencies ratio $f_{\text{RF}}/f_{\text{Opt}}$ (with $f_{\text{Opt}} \approx 192$ THz in our case).

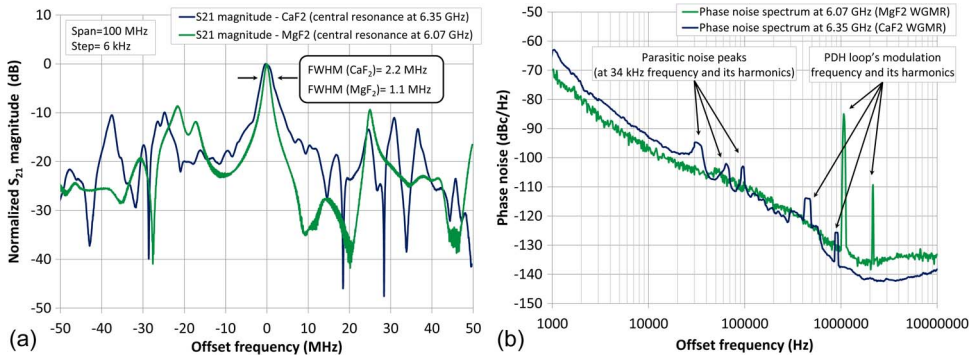

Fig. 4. (a) S_{21} coefficient's magnitude measurement focused on the modes at 6.35 GHz in the CaF_2 WGMR and at 6.07 GHz in the MgF_2 WGMR. (b) Phase noise spectra obtained when the CaF_2 WGMR and the MgF_2 WGMR are used to stabilize the oscillation frequency in an OEO setup.

In Fig. 4, a focus on the optical modes at 6.35 GHz in the CaF_2 WGMR and at 6.07 GHz in the MgF_2 WGMR has given, respectively, FWHMs of 2.2 MHz and 1.1 MHz. Therefore, WGMRs' loaded optical *Qs* of 0.9×10^8 and 1.7×10^8 can be respectively derived at a laser wavelength $\lambda = 1559$ nm. Moreover, the corresponding loaded microwave *Qs* will be, respectively, equal to 3×10^3 at 6.35 GHz and 5.4×10^3 at 6.07 GHz. By way of comparison, the $Q_{\text{RF-MgF}_2}$ is almost two times higher than the $Q_{\text{RF-CaF}_2}$. Therefore, following Leeson's approach on the phase noise in oscillators [18], [19], a theoretically lower phase noise level by 6 dB is to be expected in the white frequency noise region of the phase noise of the OEO stabilized on the MgF_2 WGMR.

From the above results, we can see that the $Q_{\text{Opt-int-CaF}_2}$ is degraded by almost 10 times against almost 4 times for the $Q_{\text{Opt-int-MgF}_2}$ when the WGMRs were included in the OEO loop (the WGMRs were loaded and no more isolated). This higher degradation in the intrinsic *Q* in the case of the CaF_2 WGMR, is due to the manual coupling control used to couple the laser lightwave to this WGMR. Aside from that, one can notice that the resonances recovered in the microwave frequency domain did not have a perfect Lorentzian shape. This is because the optical spectrum recovered in the microwave frequency domain consists of a series of overlapping resonance lines belonging to different optical resonance combs inside a WGMR.

2.2.3. Comparison of Optical Modes in the CaF_2 WGMR

As already stated, our microwave domain characterization technique allows an accurate characterization only for the modes belonging to same family of the optical mode onto which the laser wavelength is stabilized. Otherwise, the resulting recovered optical spectrum of the mode under-test will consist of an overlap between, at least, the optical resonance comb of the mode onto which the laser wavelength is stabilized and the optical resonance comb to which belong the optical mode under-test.

Using the CaF_2 WGMR, we have tried to slightly modify the OEO loop's gain bandwidth in order to characterize other optical modes generated inside this WGMR and to use them later to stabilize the oscillation frequency in an OEO. Principally, three resonances at 10.5 GHz, 11.4 GHz, and 12.7 GHz have been characterized in the same conditions as for the optical mode at 6.35 GHz: The same laser-WGMR optical coupling state and the laser wavelength was still stabilized onto the same identified optical mode of the CaF_2 WGMR [see Fig. 5(a)].

The focus on the abovementioned three optical modes under-test has given respectively FWHMs of 1.8 MHz, 1.7 MHz, and 2.2 MHz [see Fig. 5(b)]. Therefore, the loaded optical *Qs* of these modes are interestingly similar. This proves that, once a WGMR is well polished, one can get very high *Qs* for different transverse modes even if these modes do not belong to the fundamental mode's family. For instance, our fabricated WGMRs can feature surface roughness of less than 5 nm [20].

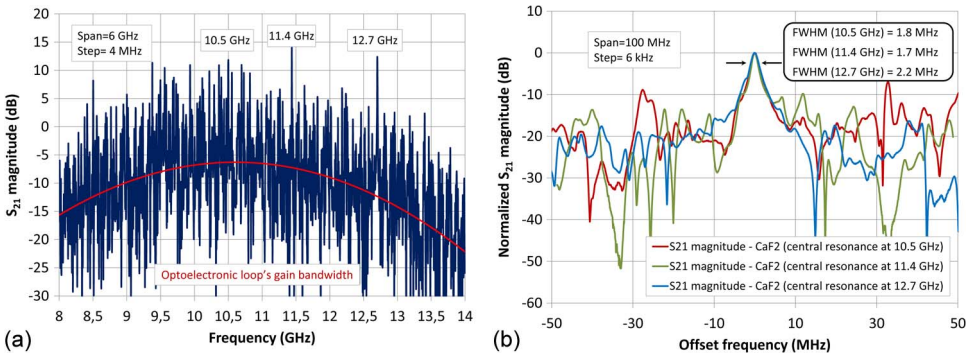

Fig. 5. S_{21} coefficient's magnitude measurement performed on the CaF_2 WGMR. (a) Large scan bandwidth measurement and (b) measurements focused on the modes at 10.5 GHz, 11.4 GHz, and 12.7 GHz.

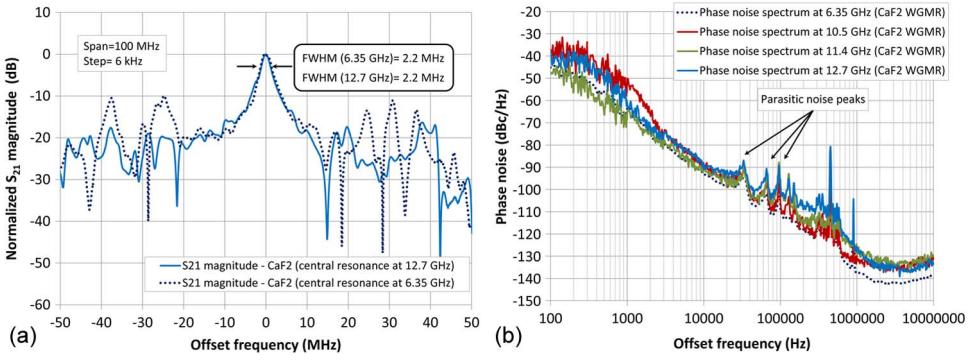

Fig. 6. (a) S_{21} coefficient's magnitude measurement focused on the modes at 6.35 GHz and 12.7 GHz in the CaF_2 WGMR. (b) Phase noise spectra obtained when different modes of the CaF_2 WGMR are used to stabilize the oscillation frequency in the OEO setup.

On the other hand, the comparison of the S_{21} coefficients obtained for the resonances at 6.35 GHz and 12.7 GHz shows that the same FWHM is obtained [see Fig. 6(a)]. This further proves that these two modes belong to the same resonance comb in the CaF_2 WGMR. Far from the two resonances' centers, the dissimilarity in shapes is due to a "Vernier effect" in the recovered optical spectrum, consisting of many overlapping optical resonance combs featuring various *FSRs* [21]. Additionally, it is noteworthy that, for the modes at 10.5 GHz and 11.4 GHz, the resulting recovered optical spectrum of the mode under-test consisted in both cases of an overlap between, at least, the optical resonance comb of the mode onto which the laser wavelength was stabilized and the optical resonance comb to which belong the optical mode under-test. Yet, the results obtained for both modes under-test still prove our assumption on the possibility of obtaining very high *Qs* for different transverse modes belonging to different resonance combs generated in a well-polished WGMR.

3. Characterization of the Optoelectronic Oscillator

From the above results, it was interesting to compare the phase noise performance of the OEO when it is stabilized on the different studied optical modes. Therefore, experimental RF and phase noise spectra measurements have been performed on our OEO for the different cases. These measurements have been accomplished using a Rohde & Schwarz FSW50 electrical signal and spectrum analyzer (ESSA).

For both modes at 6.35 GHz and 6.07 GHz, respectively, generated in the CaF_2 WGMR and the MgF_2 WGMR, the OEO loop has been closed after gain and phase adjustments. The

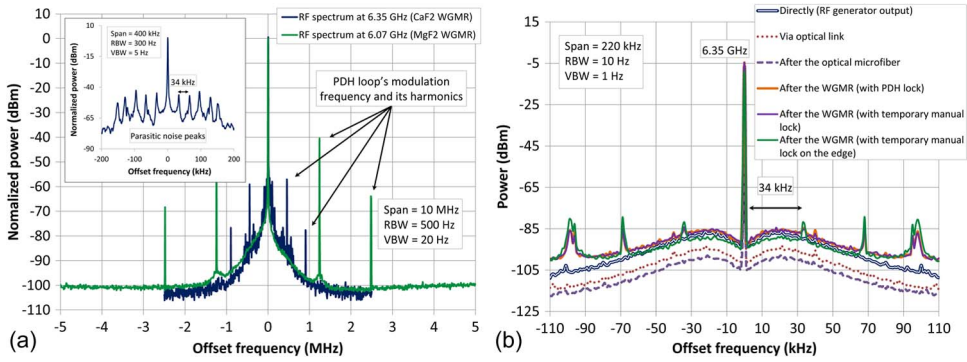

Fig. 7. (a) Comparison of the oscillation RF spectra of the OEO when both modes at 6.35 GHz and 6.07 GHz, respectively, generated in the CaF_2 WGMR and the MgF_2 WGMR, are used (the inset figure shows the excess noise peaks generated in the RF spectrum of the OEO based on the CaF_2 WGMR). (b) RF spectrum of an RF synthesizer signal at 6.35 GHz: directly measured and then again measured after its transmission through an optical link (the OEO setup in open loop configuration) in different configurations.

oscillation spectra for both cases are given in Fig. 7(a). In the RF spectrum of the OEO based on the CaF_2 WGMR, excess noise peaks at a 34 kHz frequency and its harmonics were generated near the oscillation frequency and beside the PDH loop's modulation sidebands [see the inset figure in Fig. 7(a)]. Further investigations, detailed in the next section, have been performed to determine the origin of such parasitic noise peaks.

Likewise, phase noise spectrum measurements for both OEOs, at 6.35 GHz and 6.07 GHz, have been performed using the ESSA. The resulting phase noise spectra are presented in Fig. 4(b). In these spectra, we can clearly notice the 4 dB lower phase noise level (a 6 dB lower level was theoretically expected) in the white frequency noise region obtained for the OEO stabilized on the MgF_2 WGMR, even though the MgF_2 WGMR's $Q_{Opt\text{-}int}$ was lower. Indeed, the MgF_2 WGMR had on the other hand almost two times higher loaded Q_{Opt} obtained thanks to an accurate laser-WGMR optical coupling.

The oscillation phase noise spectra of the OEO have been recorded and compared when the different studied modes generated inside the CaF_2 WGMR have been used to stabilize the oscillation frequency in the OEO. The phase noise spectra are given in Fig. 6(b) and they show comparable phase noise levels.

4. Investigations on the Excess Noise Peaks

4.1. Origin of Close-in Spurious Peaks

We have performed dedicated measurements in order to identify the origin of the excess noise peaks observed in the oscillation spectrum of the OEO at 6.35 GHz. For this purpose, we have directly measured the RF spectrum of an RF synthesizer signal at 6.35 GHz and later measured its RF spectrum when the signal is transmitted through an optical link. This optical link was nothing more than the open loop architecture of the OEO. In that case, different RF spectra were recorded using the ESSA in different configurations: after the optical microfiber and after the CaF_2 WGMR. When the CaF_2 WGMR was added, we have recorded the transmitted RF signal's spectrum as follows: when the laser was locked onto the optical resonance center using the PDH technique or manually (temporarily, to see if the PDH loop was responsible of these noise peaks), and when the laser was manually locked on the resonance edge. The different recorded RF spectra are depicted in Fig. 7(b). The recorded spectra show that the noise peaks arise when the WGMR is added into the optical link. This suggests that the noise peaks are likely to be generated inside the CaF_2 WGMR. On the other hand, one can notice that the noise peaks becomes higher when the laser is locked onto the edge of the optical resonance, suggesting that the noise peaks are likely due to a laser frequency noise converted into

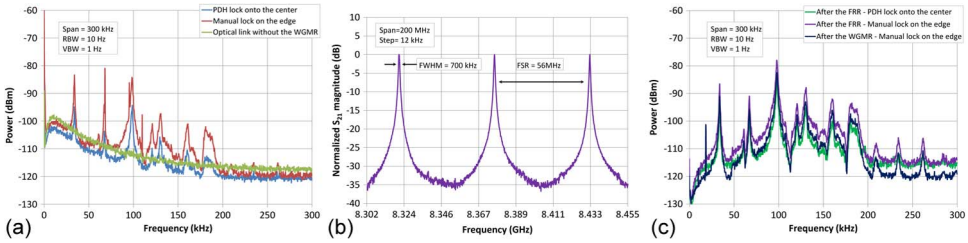

Fig. 8. (a) Low frequency (DC) spectra of a transmitted unmodulated laser signal through an optical link (the OEO setup in open loop configuration) without the CaF_2 WGMR and then when the CaF_2 WGMR was added. (b) S_{21} coefficient's magnitude measurement focused on modes generated in a 4m-long FRR. (c) Same tests performed as in (a) when the CaF_2 WGMR has been replaced by the FRR (a DC-block has been added to protect the ESSA).

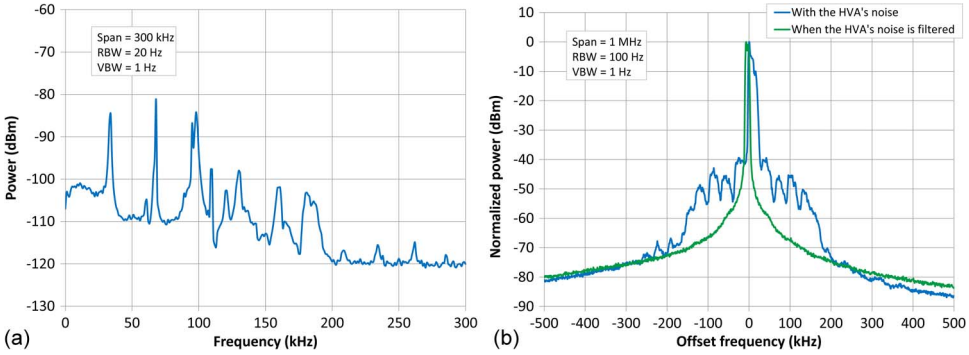

Fig. 9. (a) Low frequency (DC) spectrum measured at the output of the HVA (when no input signal is added). (b) Recorded RF spectra for the OEO, showing the up-converted HVA's noise folded onto the OEO's generated RF signal.

amplitude noise inside the WGMR. The above results have been also confirmed when the fast photodiode has been replaced by a slow photodiode to detect the low frequency (DC) part of a transmitted unmodulated laser carrier through the same optical link [see Fig. 8(a)].

In further investigations, the CaF_2 WGMR has been replaced by a high-Q ($Q_{Opt} \approx 0.3 \times 10^9$) 4m-long fiber ring resonator (FRR) [see Fig. 8(b)]. The FRR has been chosen because of its simplicity and its similarity with the WGMR, especially regarding the resonance conditions [22]. Using the FRR, we have obtained similar results as the CaF_2 WGMR case but with slightly higher noise peaks when the laser is locked on the edge of the resonance [see Fig. 8(c)]. This further supports the second suggestion of a converted laser frequency noise inside the resonator because the FRR has a much higher Q_{Opt} than the CaF_2 WGMR.

After several individual tests performed on the different components included inside the OEO setup, we have found that the noise peaks were generated by the high voltage amplifier (HVA) used in the PDH loop to amplify the PDH loop's control signal. This control signal is sent to the laser's piezoelectric transducer to control its wavelength regarding the optical resonance [see Fig. 2(a)]. Indeed, the same spectral shape, including noise peaks at the same frequencies of those observed in the OEO spectrum, was obtained when the RF spectrum of what should be a perfect DC signal at the amplifier's output has been measured [see Fig. 9(a)].

Subsequently, we have recorded the OEO's RF spectrum in presence of the HVA's noise and when the HVA's noise has been efficiently filtered (by adding a high-voltage low pass filter at the HVA's output). The recorded RF spectra are presented in Fig. 9(b). They show undoubtedly how the HVA's noise is up-converted and folded onto the OEO's generated RF signal, therefore degrading its spectral purity.

From the different aforementioned investigations, we can imply that the HVA's noise was most likely frequency modulating the laser carrier via the laser's piezoelectric transducer. Later

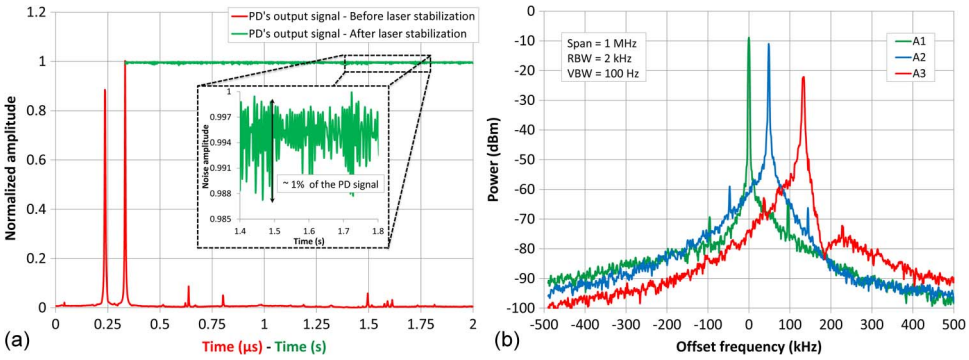

Fig. 10. (a) Normalized transmitted laser signal through a WGMR, detected by a slow photodiode and recorded by an oscilloscope (in red; time scale in microseconds), while scanning the laser wavelength and (in green; time scale in second) when the laser wavelength was stabilized onto the center of the optical resonance using the PDH loop. (b) Multiple acquisitions of FRR-based OEO's RF spectrum taken while slightly shifting the laser carrier from the center of the optical resonance (by less than 5%) to witness the rapid evolution and degradation of the OEO's RF spectrum caused by the inappropriate setting of the PDH loop's parameters.

on, this frequency modulation was converted into amplitude modulation via the optical resonator, especially when the laser carrier was not stabilized onto the center of the optical resonance. In addition, this proves the complexity of the OEO system where each noise contribution, even when originating from marginal components in the OEO setup, can induce a drastic deterioration of the OEO's spectral purity.

4.2. Effects of the PDH Laser Stabilization Loop

From the previous section, we can see that an appropriate setting of the PDH loop's parameters is very critical for our OEO setup. Otherwise, the laser will not be well stabilized onto the center of the optical resonance and this may therefore amplify some noise conversion phenomena occurring inside the OEO loop. Moreover, even when no excess noise is present in the OEO loop, an unsuitable setting of the PDH loop's parameters may severely affect the OEO performance.

In Fig. 10(a), we present the normalized transmitted laser signal through a WGMR, detected by a slow photodiode and recorded by an oscilloscope while scanning the laser wavelength. Some of the optical modes generated inside the WGMR are shown. When the laser carrier was stabilized onto the center of one of these optical modes using the PDH loop, long term stability and low noise performance have been achieved for the stabilized laser carrier and, therefore, for the OEO.

On the other hand, when the laser wavelength was intentionally slightly shifted from the center of the optical resonance (by less than 5%), we have found that the RF spectrum of the WGMR-based OEO shifted rapidly and that its spectral purity was degraded. In order to be sure that this OEO's spectral purity degradation was only due to the laser wavelength shift from the resonance center and not to the non-Lorentzian shape of the recovered optical mode we were using, the same experiment has been repeated using the aforementioned FRR. Indeed, besides its similarity with a WGMR, especially regarding the resonance conditions, it is possible to generate a single transverse optical resonance comb in a FRR (if the input light's polarization is well managed) [22]. Therefore, the recovered optical spectrum in the microwave domain will only consist of this single transverse resonance comb (no overlapping behavior is obtained compared to the WGMR case). As a result, almost Lorentzian-shape and similar resonances are recovered in the microwave frequency domain [see Fig. 8(b)].

Multiple acquisitions of the RF spectrum of the FRR-based OEO have been recorded while slightly shifting the laser wavelength from the resonance center. The obtained results, presented in Fig. 10(b), confirm that the spectral purity degradation in the FRR-based OEO and

the WGMR-based OEO is exclusively due to the laser wavelength shift from the resonance center in that case. Moreover, these additional results further prove the importance of accurate laser carrier stabilization onto the center of an optical resonance in an optical resonator-based OEO.

5. Conclusion

In this article, we have investigated the performance of an OEO based on two different monocrystalline disk-shaped WGMRs (CaF_2 and MgF_2). First, the performance of the two WGMRs have been compared to prove the importance of an accurate laser lightwave coupling into and out of the WGMR when the WGMR is meant to be used as the stability element inside an OEO. This accurate coupling was performed in order to take full advantage of the WGMR's high intrinsic quality factor. Subsequently, we have studied the performance of the OEO when different modes belonging to different resonance combs of the CaF_2 WGMR have been used. This has been made to prove that once a WGMR is well polished, one can get very high *Qs* for different transverse modes, even if they do not belong to the fundamental modes' family, and therefore good performance can be obtained in the OEO. In addition, some close-in phase noise peaks were found to be generated in the OEO spectrum. The origin of these noise peaks has been identified and the noise peaks were finally reduced. This emphasizes the complexity of an OEO system where each noise contribution can severely degrade the phase noise performance. Finally, we have proven that an inappropriate setting of the parameters of the laser stabilization loop could drastically affect the performance of an optical resonator-based OEO.

References

[1] L. Maleki, "Sources: The optoelectronic oscillator," *Nature Photon.*, vol. 5, no. 12, pp. 728–730, Dec. 2011.
[2] L. Maleki, "The opto-electronic oscillator (OEO): Review and recent progress," in *Proc. IEEE EFTF*, Apr. 2012, pp. 497–500.
[3] D. Eliyahu, D. Seidel, and L. Maleki, "RF amplitude and phase-noise reduction of an optical link and an opto-electronic oscillator," *IEEE Trans Microw. Theory Techn.*, vol. 56, no. 2, pp. 449–456, Feb. 2008.
[4] K. Volyanskiy, Y. K. Chembo, L. Larger, and E. Rubiola, "Contribution of laser frequency and power fluctuations to the microwave phase noise of optoelectronic oscillators," *J Lightw. Technol.*, vol. 28, no. 18, pp. 2730–2735, Sep. 2010.
[5] O. Okusaga *et al.*, "Optical scattering induced noise in RF-photonic systems," in *Proc. IEEE IFCS Eur. Freq. Time Forum*, May 2011, pp. 1–6.
[6] A. Docherty, C. R. Menyuk, O. Okusaga, and Z. Weimin, "Stimulated Rayleigh scattering and amplitude-to-phase conversion as a source of length-dependent phase noise in OEOs," in *Proc. IEEE IFCS*, May 2012, pp. 1–5.
[7] O. Okusaga, W. Zhou, J. Cahill, A. Docherty, and C. R. Menyuk, "Fiber-induced degradation in RF-over-fiber links," in *Proc. IEEE IFCS*, May 2012, pp. 1–5.
[8] D. Eliyahu and L. Maleki, "Low phase noise and spurious level in multi-loop optoelectronic oscillators," in *Proc. IEEE Int. Freq. Control Symp.*, May 2013, pp. 405–410.
[9] O. Okusaga *et al.*, "Spurious mode reduction in dual injection-locked optoelectronic oscillators," *Opt. Express*, vol. 19, no. 7, pp. 5839–5854, Mar. 2011.
[10] A. A. Savchenkov *et al.*, "Whispering-gallery mode based opto-electronic oscillators," in *Proc. IEEE Conf. Freq. Cont. Symp.*, Jun. 2010, pp. 554–557.
[11] K. Volyanskiy *et al.*, "Compact optoelectronic microwave oscillators using ultra-high Q whispering gallery mode disk-resonators and phase modulation," *Opt. Express*, vol. 18, no. 21, pp. 22 358–22 363, Oct. 2010.
[12] P. Merrer *et al.*, "Characterization technique of optical whispering gallery mode resonators in the microwave frequency domain for optoelectronic oscillators," *Appl. Opt.*, vol. 51, no. 20, pp. 4742–4748, Jul. 2012.
[13] A. Coillet *et al.*, "Time-domain dynamics and stability analysis of optoelectronic oscillators based on whispering-gallery mode resonators," *IEEE J. Sel. Topics Quantum Electron*, vol. 19, no. 5, pp. 1–12, Sep. 2013.
[14] A. Coillet *et al.*, "Microwave photonics systems based on whispering-gallery-mode resonators," *J. Vis. Exp.*, vol. 78, p. 50 423, Aug. 2013.
[15] G. Lin *et al.*, "Excitation mapping of whispering gallery modes in silica microcavities," *Opt. Lett.*, vol. 35, no. 4, pp. 583–585, Feb. 2010.
[16] Y. Dumeige *et al.*, "Determination of coupling regime of high-Q resonators and optical gain of highly selective amplifiers," *J. Opt. Soc. Am. B*, vol. 25, no. 12, pp. 2073–2080, Dec. 2008.
[17] E. Black, "An introduction to Pound-Drever-Hall laser frequency stabilization," *Am. J. Phys.*, vol. 69, no. 1, pp. 79–87, Jan. 2001.
[18] D. B. Leeson, "A simple model of feedback oscillator noise spectrum," *Proc. IEEE*, vol. 54, no. 2, pp. 329–330, Feb. 1966.

[19] A. Bouchier, K. Saleh, P. H. Merrer, O. Llopis, and G. Cibiel, "Theoretical and experimental study of the phase noise of opto-electronic oscillators based on high quality factor optical resonators," in *Proc. IEEE Int. Freq. Cont. Symp.* Jun. 2010, pp. 544–548.
[20] G. Lin, S. Diallo, R. Henriet, M. Jacquot, and Y. K. Chembo, "Barium fluoride whispering-gallery-mode disk-resonator with one billion quality-factor," *Opt. Lett.*, vol. 39, no. 20, pp. 6009–6012, Oct. 2014.
[21] P. Saeung and P. P. Yupapin, "Vernier effect of multiple-ring resonator filters modeling by a graphical approach," *Opt. Eng.*, vol. 46, no. 7, p. 075005, Jul. 2007.
[22] K. Saleh, O. Llopis, and G. Cibiel, "Optical scattering induced noise in fiber ring resonators and optoelectronic oscillators," *J Lightw. Technol.*, vol. 31, no. 9, pp. 1433–1446, May 2013.